Nanoscale

PAPER

View Article Online
View Journal | View Issue

Cite this: *Nanoscale*, 2025, **17**, 9363

An organic solvent-free self-assembly strategy for scalable preparation of nanobiopesticides with enhanced insecticidal activity against houseflies†

Huiping Chen,[a] Zhifei Yang,[a] Qing Yin,[b] Wenjie Shangguan,[a] Chong Cao,[a] Qiliang Huang[a] and Lidong Cao *[a]

The abuse of toxic organic solvents has caused great harm to human health and the environment. Therefore, developing an environmentally friendly nano-based pesticide formulation without using harmful solvents is urgent to improve the efficacy of pesticides and minimize environmental and health risks. Herein, by combining aspartic acid (Asp) with spinosad (SSD) as an attractive building unit, a self-assembly and carrier-minimized strategy was applied to construct a nanobiopesticide (Asp-SSD) simultaneously. To further improve the storage stability of the formulation, the biogenic surfactant alkyl polyglucoside (APG) was subsequently added to afford a more stable and smaller nano-delivery system (Asp-SSD-APG). Bioactivity assays showed that Asp-SSD-APG exhibited good quick-acting performance against *Musca domestica* in the spray assay, and the insecticidal activities of Asp-SSD and Asp-SSD-APG were better than that of the SSD nano-suspension concentrate (Nano-SC). Compared to CK, Asp-SSD-APG reduced the activity of GST, SOD, and CAT in *M. domestica*, which contributed to the enhanced insecticidal effect of SSD. The cell viability evaluation in 4T1 cells showed that Asp-SSD-APG posed a low risk to the mammalian cells. This study provides an alternative approach for developing environmentally benign nanobiopesticides with a self-assembly and carrier-minimized strategy, which has the potential to improve the efficacy and safety of pesticides in the public health field.

Received 6th December 2024,
Accepted 7th March 2025

DOI: 10.1039/d4nr05141f

rsc.li/nanoscale

Introduction

Musca domestica (*M. domestica*) is a cosmopolitan public health pest. It can cause annoyance and act as a mechanical carrier of pathogens such as bacteria, fungi, viruses, and other parasites that can cause different human and animal diseases.[1–3] Currently, insecticides are considered to be the most important and effective tool to reduce the spread of disease to humans by controlling *M. domestica* populations.[4] Compared with traditional chemical pesticides, biopesticides have the advantages of being biodegradable, eco-friendly, low impact on the ecological environment, and safe for humans and animals.[5]

Recently, research studies on the application of nanotechnology in pesticides have become increasingly popular.[6] The future development and application of nanopesticides are expected to improve the efficiency of pesticide utilization.[7] The guiding principles for sustainability in nanopesticide research are efficiency, safety, and circularity.[8] However, over-modified nanomaterials within nanoscale delivery platforms through complex processes and organic solvents deviate from this core principle.[9] Moreover, many nanocarriers suffered from low pesticide-loading efficiency because the nanocarriers themselves accounted for a much larger proportion of the formulation than the active ingredient.[10] Carrier-minimized nanopesticides were constructed through the molecular design of prodrugs and molecule self-assembly.[11] This is expected to address the environmental risks associated with the unrestricted introduction of nanomaterials and low pesticide-loading efficiency.[9,12] For instance, self-assembled submicron particles based on berberine and curcumin were prepared through various noncovalent interactions without using any adjuvants.[13] Tang *et al.* prepared self-assembled nanoparticles with the fungicide fenhexamid and polyhexamethylene biguanide by the electrostatic and hydrophobic interactions.[14]

Spinosad (SSD) is a biopesticide with stomach and contact poison, activating nicotinic acetylcholine receptors and inhibiting gamma-aminobutyric acid receptors in the central nervous system of insects, and can target species from several insect orders (Coleoptera, Diptera, Hymenoptera, Isoptera, Lepidoptera

[a]*State Key Laboratory for Biology of Plant Diseases and Insect Pests, Institute of Plant Protection, Chinese Academy of Agricultural Sciences, Beijing, 100193, P. R. China. E-mail: caolidong@caas.cn; Fax: +86-10-6281-6909*
[b]*Tianjin Yorkool Science and Technology Co., Ltd, Tianjin300392, P. R. China*
† Electronic supplementary information (ESI) available: See DOI: https://doi.org/10.1039/d4nr05141f

and Thysanoptera).[15–17] It is composed of a mixture of related spinosyn toxins, mainly spinosyns A and D.[18] The structure of SSD contains a tertiary amine group which makes SSD susceptible to protonation under acidic conditions.[19,20] Benefiting from the amphiphilicity of sulfamic acid and glycyrrhizic acid, Tian *et al.* and Wei *et al.* constructed SSD-sulfamic acid nanoparticles and glycyrrhizic acid-tailored SSD nanoparticles, respectively.[21,22] However, phosphate buffered saline solution and the toxic solvent methanol were used and included in this SSD formulation, which is not amicable for sanitary purposes. Hence, it's highly desirable to develop an organic solvent-free method to prepare nanobiopesticides based on the self-assembly between SSD and other small molecules, which could be applicable for *M. domestica* control.

In this study, the more cost-effective amino acid aspartic acid (Asp) with carboxylic acid groups is used as an ideal self-assembly companion for SSD.[23] Moreover, Asp, as a naturally existing compound, is expected to be biodegradable and biocompatible.[24] According to the molecular structures and physicochemical properties of SSD and Asp, Asp-tailored SSD (Asp-SSD) can spontaneously form supramolecular architectures through non-covalent bonding in aqueous solution. Formulation stability will affect pesticide efficacy. Furthermore, alkyl polyglucoside (APG), as a non-ionic surfactant with biocompatibility and biodegradability,[25,26] was used to stabilize the Asp-SSD nanoformulation. In this study, the preparation conditions were optimized by changing the mass ratio of Asp to SSD, reaction temperature and the amount of the surfactants, and the obtained self-assembly system was characterized by scanning electron microscopy (SEM), cryogenic transmission electron microscopy (Cryo-TEM), Fourier transform infrared spectroscopy (FTIR), and ultraviolet (UV) spectrophotometry. Furthermore, the stability, release properties, photodegradation behaviors, insecticidal activity against *M. domestica*, and cell viability of the obtained self-assembly system were also investigated. This study seeks to provide a novel and green method to prepare nanobiopesticides for potential application in sustainable human health protection.

Results and discussion

Preparation of spinosad nanoformulations

The water-based SSD delivery system (Asp-SSD) was prepared by dissolving Asp and SSD in water *via* stirring at a speed of 1000 rpm for 2 h. To further improve the storage stability of the formulation, surfactant APG was subsequently added to afford a more stable and smaller nano-delivery system (Asp-SSD-APG). The synthesis and proposed formation mechanism of self-assembled Asp-SSD and Asp-SSD-APG structures are illustrated in Scheme 1. In the assembly process, water-soluble Asp and hydrophobic SSD were introduced into an aqueous solution under high-speed stirring and elevated temperature conditions, and the pH of solution was determined to be 3.64 at a mass ratio of 1 : 2 (Asp to SSD) (Fig. S1†). The isoelectric point of Asp is 2.77.[27] At pH 3.64 (the mass ratio of 1 : 2 (Asp to SSD)), the carboxyl groups of Asp are partially ionized, generating negative charges (COO^-). Concurrently, the tertiary amine groups within the SSD molecules underwent protonation, facilitating the electrostatic interaction with Asp. Initially, linear macromolecular fragments were formed through electrostatic interactions between the protonated tertiary amine groups of SSD and the carboxylate groups of Asp.[21] These fragments subsequently underwent conformational changes, rotating and intertwining to form spherical, three-dimensional structures stabilized by hydrogen bonding and van der Waals force. Among them, hydrogen bonds might come from the ester groups of SSD and the amino groups of Asp, and van der Waals forces might be generated by SSD molecular skeletons.[28] In this arrangement, the hydrophobic SSD components might form the core, while the hydrophilic Asp components might constitute the shell.[22] The presence of unbound primary amine groups on Asp imparted a positive charge to the system, promoting the orderly dispersion of the core–shell structures in water. Furthermore, the incorporation of APG, a non-ionic and sugar-based surfactant, significantly influenced the stability and particle size of the co-assemblies. The adsorption of APG around the Asp-SSD structures created a steric barrier that

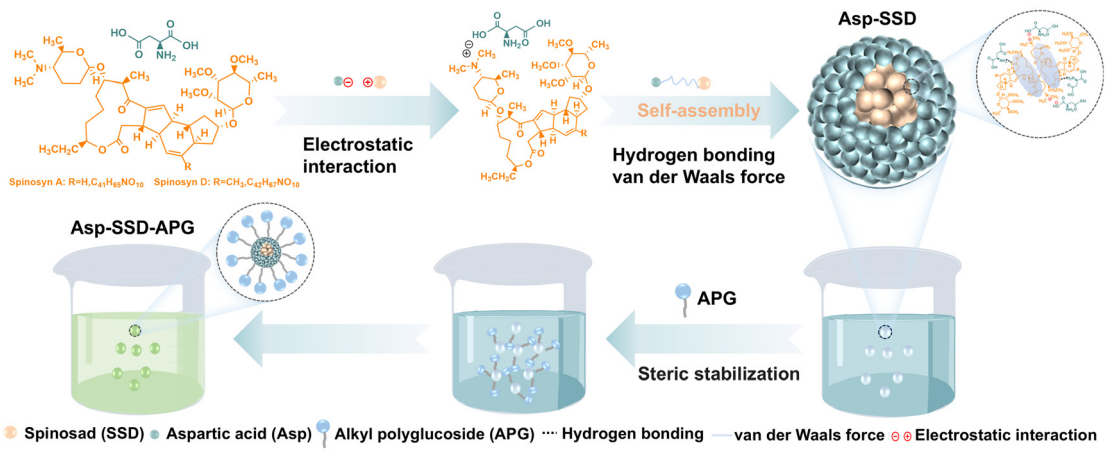

Scheme 1 Schematic illustration for the self-assembly of Asp-SSD from Asp and SSD, and the steric stabilization of APG.

effectively hindered aggregation, thereby enhancing the stability of the dispersions.[29] Additionally, the short chain length of the sugar-based surfactant facilitated more efficient packing on the Asp-SSD surface, resulting in smaller particle sizes.

The assembly rate of SSD, which represents the ratio of the initial amount of SSD to the amount of SSD in the Asp-SSD (or Asp-SSD-APG) system, was used to determine the optimized mass ratio of Asp to SSD, reaction temperature and surfactant. With the proportion of Asp increased from 1 : 4 to 1 : 1, the highest assembly rate of 95% was achieved at the mass ratio of 1 : 2 (Fig. 1a), and the reaction solution was changed from opaque (1 : 4) to clear (1 : 2) then to opaque (1 : 1). The proportion of Asp could influence the pH of the solution. Specifically, decreasing the proportion of Asp generally leads to an increase in the pH of the solution due to the lower concentration of acidic groups present (Fig. S1†). Moreover, the temperature also affected the formation of the self-assembled system. The assembly rates of Asp-SSD were positively correlated at 25 °C, 35 °C, and 45 °C, respectively. However, when the temperature was higher at 55 °C, the self-assembly rate slightly decreased (Fig. 1b). Considering the assembly rate and energy saving together, the mass ratio of Asp to SSD (1 : 2) and 35 °C were adopted as the optimum reaction conditions. The SSD content in the water-based system was 1%, which was measured by HPLC.

Surfactants play an important role in stabilizing the pesticide formulation and improving the performance of pesticides. The stability of Asp-SSD with different surfactants can be reflected by Turbiscan stability index (TSI) values. The higher the TSI value obtained, the less stable the sample.[30] According to the combined consideration of SSD assembly rate and TSI, APG was selected as the optimal surfactant for the delivery system of Asp-SSD (Fig. 1c and d). The present study was consistent with a previous study that the drug loading and TSI were also chosen as the parameters for preparation of DIF/CuS@Cu-MOF.[31] The self-assembly formation mechanism of Asp with SSD was investigated by isothermal titration calorimetry (ITC) (Fig. 1e). The SSD solution was titrated with Asp aqueous solution to determine their interaction. The high-affinity constant K_a (M^{-1}) showed a strong interaction between Asp and SSD. The negative ΔG value of −30.63 kJ mol^{-1} indicated that a spontaneous reaction occurred between Asp and SSD. The negative values of ΔH (−35.54 kJ mol^{-1}) and ΔS (−16.47 J mol^{-1} K^{-1}) indicated that the combination of Asp with SSD was through hydrogen bonding and van der Waals force.[32,33]

Characterization of the samples

Morphology characterization. When Asp and SSD were stirred by magnetic force, the amphipathic Asp spontaneously combined with SSD to form a stable spherical structure confirmed by SEM and Cryo-TEM observations (Fig. 2a and b). However, the morphology of Asp and SSD was layered and blocky, respectively (Fig. S2†), which further confirmed the successful self-assembly between Asp and SSD. The spherical structure of Asp-SSD-APG was also measured by SEM (Fig. 2c). Moreover, digital photographs of the Tyndall effect and solution states of different solutions are shown in Fig. 2d and

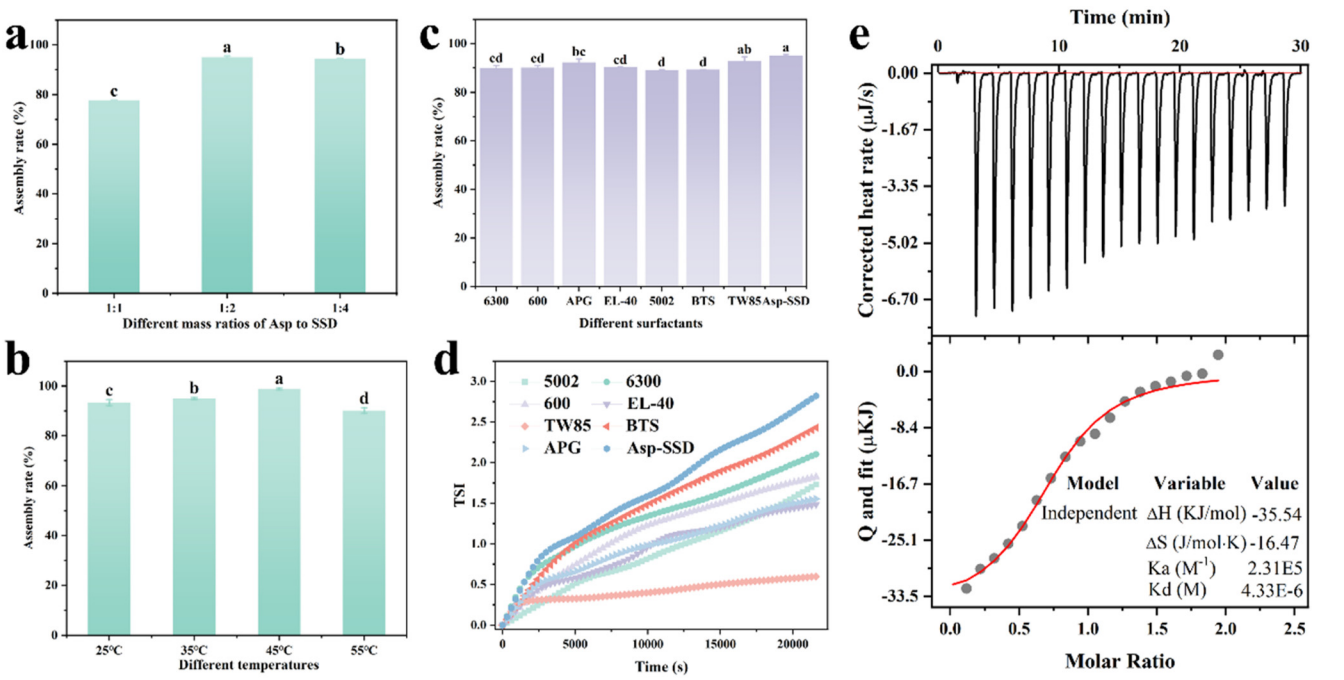

Fig. 1 Self-assembly rates of Asp-SSD at different mass ratios of Asp to SSD (a), at different temperatures (b), and with different surfactants (c); TSI values of Asp-SSD with different surfactants (d); And interaction forces between Asp and SSD in water measured by ITC (e). Bars with the same letters are not significantly different according to Tukey's *post hoc* comparisons at $P < 0.05$.

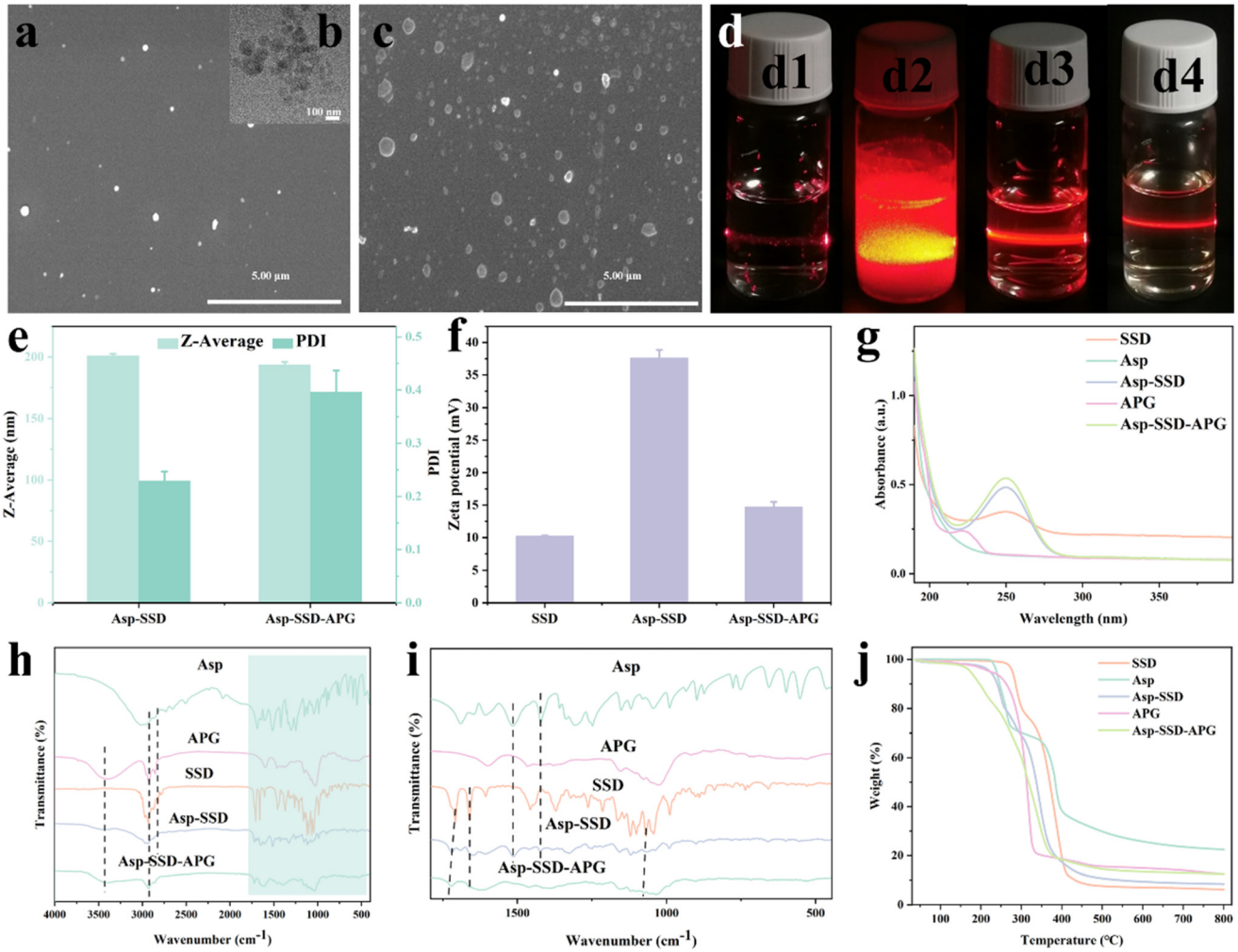

Fig. 2 Characterization of Asp-SSD and Asp-SSD-APG. The morphological characteristics by SEM (a: Asp-SSD, c: Asp-SSD-APG) and Cryo-TEM (b: Asp-SSD); Tyndall effect of different solutions (d1–d4: Asp in water, SSD in water, Asp-SSD, and Asp-SSD-APG) (d); Particle size distribution (e) and zeta potentials (f) of SSD, Asp-SSD, and Asp-SSD-APG; (g) UV spectra (g), FTIR spectra (h and i), and TGA (j) of SSD, Asp, APG, Asp-SSD, and Asp-SSD-APG. Bars show the means with standard error.

Fig. S3,† respectively. The resulting Asp-SSD and Asp-SSD-APG both exhibited a pronounced Tyndall phenomenon while Asp and SSD solutions did not produce the same phenomenon (Fig. 2d). Asp was unable to produce the Tyndall effect due to the dissolved Asp in water (Fig. 2d1), and precipitation of SSD affected light transmittance because SSD has low solubility in water (Fig. 2d2).

As shown in Fig. 2e, the particle sizes of Asp-SSD and Asp-SSD-APG were 201 nm and 194 nm, respectively. For the zeta potential, SSD with a tertiary amine group had positive charges (+10.24 mV) in water. The zeta potential of Asp-SSD increased to +37.62 mV. With the addition of the non-ionic APG, the zeta potential value decreased (+14.69 mV) (Fig. 2f), which indicated that APG might have formed an adsorption layer around Asp-SSD.

Spectral characteristics. The UV absorption spectra of SSD, Asp, APG, Asp-SSD, and Asp-SSD-APG were recorded at 190–400 nm (Fig. 2g). Asp had no maximum UV absorption in 190–400 nm. Asp-SSD and Asp-SSD-APG almost had the same UV absorption properties as SSD, and their maximum UV absorption peaks were all at 250 nm, which suggested that SSD and Asp spontaneously formed supramolecular structures through non-covalent interactions.[13] Meanwhile, APG with the maximum UV absorption peaks at 223 nm had no obvious effect on the system.

To observe the functional group information of the samples, the FTIR spectra of SSD, Asp, APG, dried Asp-SSD and Asp-SSD-APG were studied (Fig. 2h and i). The absorption peaks at 2930 and 2822 cm^{-1} for SSD were ascribed to the C–H stretching vibration, and the peaks at 1708, 1660, 1261, and 1067 cm^{-1} of SSD were attributed to the C═O stretching of O–C═O, the C═O stretching of C═C–C═O, the C–O stretching of O═C–C–O, and –$N(CH_3)_2$, respectively.[21,22,34] The absorption peak at 1510 cm^{-1} for Asp was attributed to the stretching vibration of the CO_2^-. Overall, the characteristic absorption peaks of Asp-SSD were consistent with those of Asp and SSD. The high-frequency region (3400–3200 cm^{-1}) of APG corre-

sponded to the O–H stretching,[35] and Asp-SSD-APG was also observed. The peak of C=O stretching of O–C=O on SSD shifted from 1708 cm^{-1} to a higher wavenumber of 1722 cm^{-1} in Asp-SSD, which was possibly ascribed to hydrogen bonding between SSD and Asp.[22]

Thermogravimetric analysis. TGA can characterize the thermal stability of a substance. The weight losses of Asp, SSD, Asp-SSD, APG, and Asp-SSD-APG were 66.88%, 91.19%, 87.68%, 83.14%, and 83.87% in the temperature range of 30–450 °C, respectively (Fig. 2j). This result showed that the self-assembly could improve thermal stability between SSD and Asp, and APG could also help to increase the thermal stability of the system.

Stability evaluation. The stability of pesticide formulations contributes to improving pesticide utilization. Under different conditions such as temperature, humidity, light, and dilution, the physical and chemical properties of pesticides will change (Fig. 3a), which should be carefully considered during the preparation and use process of pesticide formulations.

Storage stability assessment. To ensure the effectiveness of pesticides during a certain storage period, the pesticide formulations should have good storage stability. Asp-SSD and Asp-SSD with different surfactants were stored at different temperatures (0, 25, and 54 °C) for 7 and 14 days, respectively, to assess the storage stability (Fig. S4†). The result illustrated that Asp-SSD without surfactants at 54 °C could not prevent the aggregation and stratification of pesticides. With the addition of the non-ionic APG, Asp-SSD-APG appeared as a pale yellow and transparent liquid at 54 °C for 14 days (Fig. 3b). As shown in Fig. S5,† the average particle size of Asp-SSD (250.90 ± 1.47 nm) and Asp-SSD-APG (185.38 ± 5.20 nm) remained notably diminutive, and both systems sustained their transparency for a duration of 7 days at 0 °C. Upon subjecting Asp-SSD to a 14-day period at 54 °C, the system exhibited phenomena of aggregation and stratification of pesticides. Additionally, the system's lack of homogeneity posed challenges to the accurate measurement of particle size. Remarkably, for Asp-SSD-APG for 14 days at 54 °C, the system was still transparent and the particle size significantly decreased to 3.67 ± 0.02 nm, which was possibly due to the disruption of the initially formed self-assemblies of Asp-SSD-APG and subsequent formation of nanomicelles confirmed by the obvious Tyndall effect (Fig. S5†). As mentioned above, the higher temperature could decrease the assembly rate. In the present system, the concentration of APG was 2%, significantly exceeding its critical

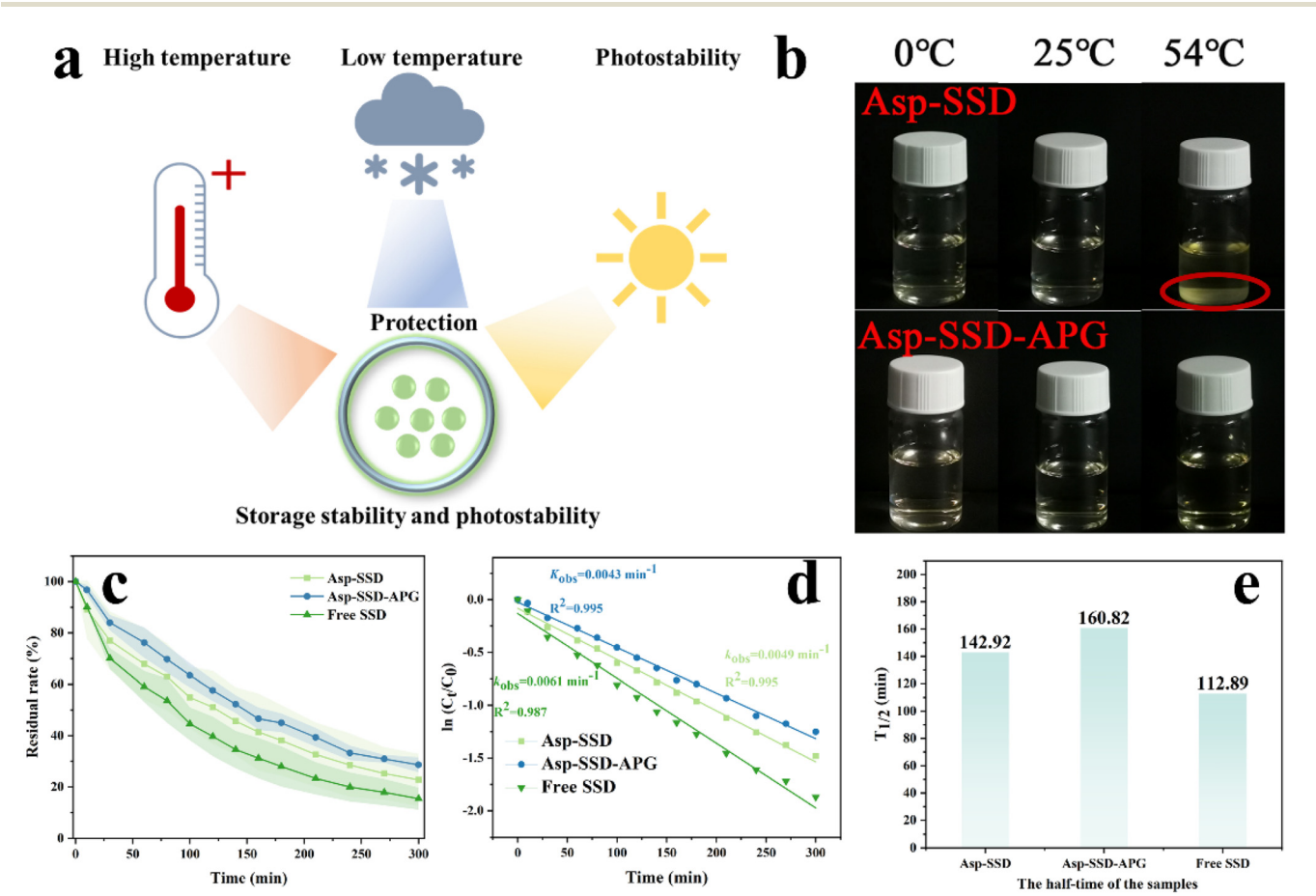

Fig. 3 Schematic illustration of storage stability and photostability of Asp-SSD and Asp-SSD-APG (a); Appearance of Asp-SSD and Asp-SSD-APG after storage at different temperatures (0, 25, and 54 °C) for 7 and 14 days (b); the residual rate (c), fitted curves (d), and half-time (e) of Asp-SSD, Asp-SSD-APG, and free SSD under UV illumination for 300 min.

micelle concentration of 0.0104 wt%,[36] facilitating the micelle formation to solubilize SSD. Although the microstructure of the solution changed for 14 days at 54 °C, the chemical stability of the active ingredient SSD was maintained, as evidenced by the almost unchanged content of 0.98% after storage. The dilution stability of Asp-SSD-APG was studied with different dilution concentrations of SSD from 80 to 5000 mg L^{-1}. The results showed that Asp-SSD-APG exhibited favorable dilution stability with a particle size range of 144.77–192.99 nm (Fig. S6†). The variations in PDI under different dilution ratios might be attributed to aggregation effects. At lower dilution ratios, increased particle concentrations reduce interparticle distances and enhance particle–particle interactions,[37,38] promoting aggregation and broadening the particle size distribution, which might lead to higher PDI values. Despite these variations, the PDI remained below 0.5, indicating relatively narrow size distributions and good stability. This stability is crucial for maintaining the performance of Asp-SSD-APG in practical applications.

Photostability evaluation. Photostability has a vital impact on the long-term control efficacy of pesticide formulations especially for photo-sensitive pesticides such as SSD. The photostability of SSD in Asp-SSD and Asp-SSD-APG was studied under UV irradiation at 500 W using free SSD as a control. The results demonstrated that the degradation rate of free SSD was higher than those of Asp-SSD and Asp-SSD-APG (Fig. 3c). The half-time ($t_{1/2}$) of Asp-SSD, Asp-SSD-APG, and free SSD for the pseudo-first-order kinetics was calculated to be 142.92, 160.82, and 112.89 min, respectively (Fig. 3d and e). Asp-SSD and Asp-SSD-APG could delay the degradation of SSD under illumination. The interaction between SSD and Asp might prevent its structure from being rapidly degraded.

Interfacial performance of Asp-SSD and Asp-SSD-APG

The wettability was determined by measuring the surface tension and contact angle. Compared to CK (pure water), SK (0.1% Tween-80 solution) and Asp solution, the surface tension of Asp-SSD decreased significantly to 40.18 mN m^{-1} (Fig. 4a). APG can effectively reduce the interfacial tension.[39] After the addition of APG, the surface tension of Asp-SSD was further decreased (31.28 mN m^{-1}), which was much lower than those of Nano-SC and free SSD (with 0.1% Tween-80 solution) (Fig. 4a). In addition, on the PTFE hydrophobic film, although the contact angle of Asp-SSD-APG was smaller than those of Nano-SC and free SSD, there was no significant difference among them (Fig. 4b).

In vitro release behavior

The release behaviors of Asp-SSD and Asp-SSD-APG were investigated in stimulated release media with different pH values. Asp-SSD and Asp-SSD-APG both demonstrated acid-sensitive properties and showed a trend of initial burst release and then sustained release (Fig. 4c). The cumulative release amount of SSD from Asp-SSD was 88.44% at pH 5 and 74.47% at pH 7 after 72 h, higher than 29.40% at pH 9. Similarly, the cumulative release of SSD from Asp-SSD-APG after 72 h was 88.36%

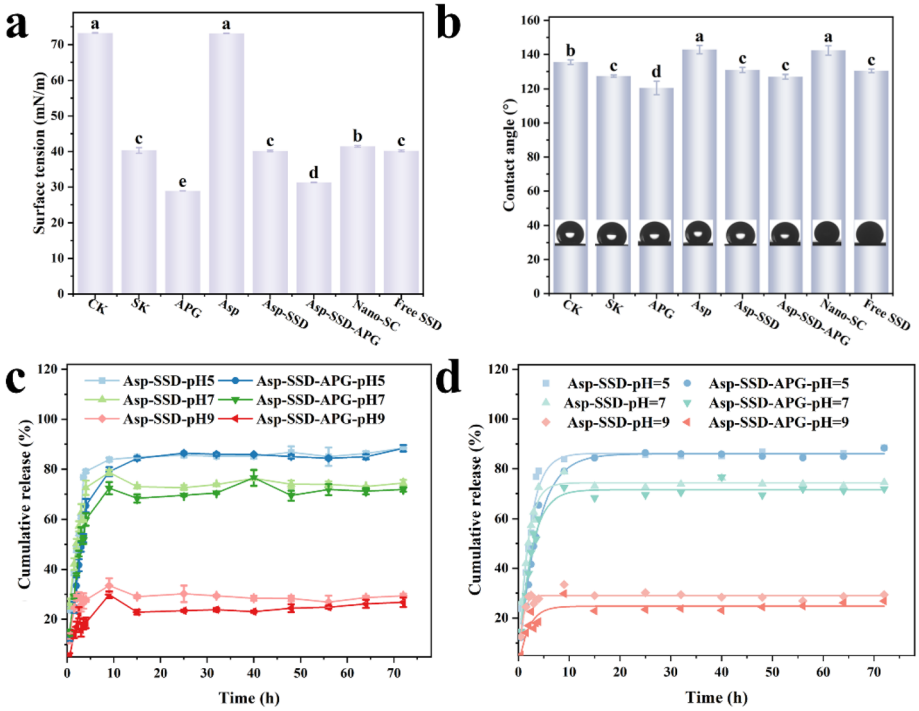

Fig. 4 Surface tensions (a) and contact angles (b) of CK (water), SK (0.1% Tween-80 solution), APG, Asp, Asp-SSD, Asp-SSD-APG, Nano-SC and free SSD (with 0.1% Tween-80 solution). Cumulative release curves (c) and fitted plots with a first-order model (d) of Asp-SSD and Asp-SSD-APG at pH values of 5, 7, and 9.

(pH 5), 71.86% (pH 7), and 26.83% (pH 9). Compared to pH 7 and pH 9, Asp had a more protonated state in an acidic environment, which led to a weaker electrostatic binding capacity between Asp and SSD,[40] thus facilitating the release of SSD. Under alkaline conditions, the release of SSD was inhibited probably because of the amino groups of SSD and Asp.[41] Moreover, compared to Asp-SSD, APG slightly delayed the release of SSD in a neutral and alkaline environment for Asp-SSD-APG. As shown in Fig. 4d, the release behavior was more consistent with the first-order model compared with the zero-order, Higuchi, and Korsmeyer-Peppas model. The correlation coefficients of Asp-SSD at pH levels of 5, 7, and 9 were 0.9617, 0.9511, and 0.8422, respectively. For Asp-SSD-APG, the first-order kinetic model was best matched with its release behavior, with high correlation coefficients of 0.9886, 0.9791, and 0.8081 at pH 5, 7, and 9, respectively. This kinetic model showed that SSD release was proportional to the concentration of the active ingredient in both systems.

Insecticidal activity assays

The insecticidal activity of the SSD formulation against *M. domestica* was evaluated using two different methods of direct spray (Fig. 5a) and residual spray (Fig. 5d).

Direct spray. The insecticidal efficiency of Asp-SSD and Asp-SSD-APG was investigated using *M. domestica* as a model insect, with 3.5% SSD nano-suspension concentration (Nano-SC, self-prepared) as the control. The aqueous solution of Asp had no insecticidal activity against *M. domestica*. Fig. 5b shows the digital images of knocked down *M. domestica* treated with Asp-SSD, Asp-SSD-APG and Nano-SC. As shown in Fig. 5c, the KT_{50} values of Asp-SSD, Asp-SSD-APG, and Nano-SC were 4.577, 3.208, and 3.441 h, respectively. The KT_{50} values of

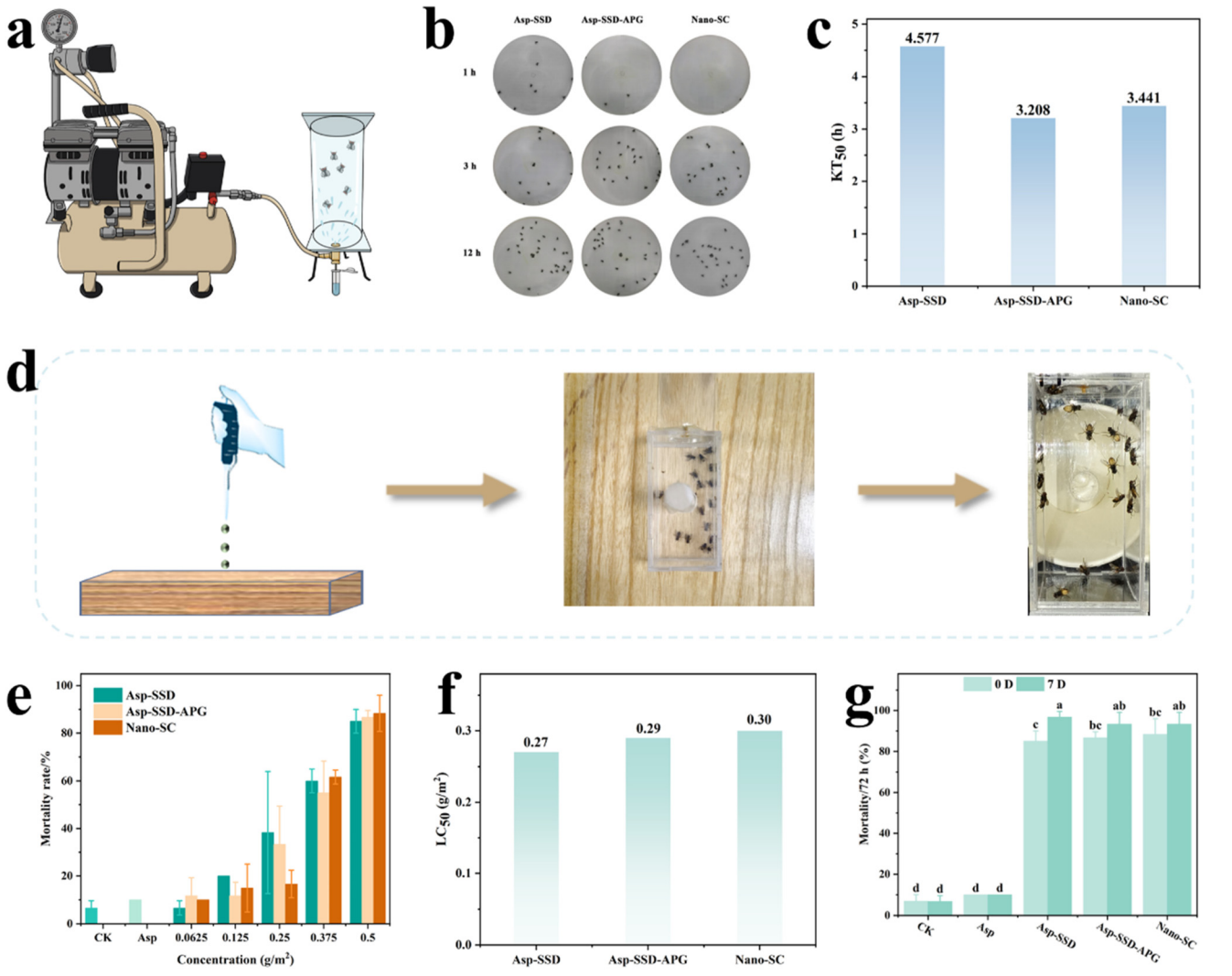

Fig. 5 Schematic illustration of direct spray (a). The digital images of knocked down *M. domestica* treated with Asp-SSD, Asp-SSD-APG and Nano-SC by the direct spray method (b). The KT_{50} values of Asp-SSD, Asp-SSD-APG and Nano-SC by the direct spray method (c). Schematic illustration of residual spray (d). The mortality rate of *M. domestica* treated with Asp-SSD, Asp-SSD-APG and Nano-SC under different concentrations of SSD (e). The LC_{50} values of Asp-SSD, Asp-SSD-APG and Nano-SC under residual spray assays (f). The mortality rate of *M. domestica* for 0 and 7 days at a concentration of 0.5 g m^{-2} (g). Bars with the same letters are not significantly different according to Tukey's *post hoc* comparisons at $P < 0.05$.

Nano-SC were higher than that of Asp-SSD-APG, but lower than that of Asp-SSD. Moreover, all *M. domestica* were dead after the treatment with SSD formulation for 24 h. These results indicated that Asp-SSD-APG had a higher insecticidal activity against houseflies.

Residual spray. To further demonstrate the insecticidal activity of Asp-SSD and Asp-SSD-APG in public hygiene, the bioassay of Asp-SSD and Asp-SSD-APG against *M. domestica* was also conducted using the residual spray method (Fig. 5d). A wooden plate surface without pesticide was used as the blank control (CK). The mortality rate of CK and aqueous solution of Asp did not exceed 10%. Fig. 5e shows that the mortality rate of *M. domestica* was positively correlated with the concentration of SSD. As the concentration of the active ingredient increased, the mortality rate of *M. domestica* improved. The LC_{50} values of the samples were 0.27 (Asp-SSD), 0.29 (Asp-SSD-APG), and 0.30 (Nano-SC) g m^{-2}, respectively (Fig. 5f). In addition, after 7 days, the mortality rate was observed to be greater than 90% for all the three treatments (Fig. 5g), indicating that Asp-SSD, Asp-SSD-APG, and Nano-SC had a longer-lasting insecticidal activity.

Enzyme activity assays

Organisms are equipped with their physiological defense to cope with environmental stress. Due to the low solubility of SSD in water, 0.1% Tween-80 solution was used as its solvent. Asp-SSD, Asp-SSD-APG, and free SSD (with 0.1% Tween-80 solution) were used for *M. domestica*, and water (CK) and 0.1% Tween-80 solution (SK) were set as the controls. Fig. 6a shows a schematic diagram of enzyme activities in the control of *M. domestica*. Fig. 6b–d show that the enzyme activities of CAT, SOD, and GST are influenced by the presence of SSD in different ways. According to Tukey's *post hoc* comparisons, the GST activity was statistically significantly decreased by 25.15% (Asp-SSD), 29.46% (Asp-SSD-APG), and 5.57% (free SSD) in *M. domestica* after exposure to the active ingredient at a concentration of 0.25 g m^{-2} when compared to CK ($P < 0.05$). After exposure to a low concentration of Asp-SSD, Asp-SSD-APG, and free SSD (0.0625 g m^{-2}), significant difference in the GST activity was observed on free SSD when compared to Asp-SSD and Asp-SSD-APG (Fig. 6b). This result showed that Asp-SSD and Asp-SSD-APG had a certain degree of inhibitory effect on the GST activity of *M. domestica*. The decrease in detoxification enzyme activity may affect the detoxification metabolism of SSD in *M. domestica*, thus increasing the toxic effect of SSD on *M. domestica*.

The SOD activity was induced after 72 h exposure of Asp-SSD with the increase in the concentration of SSD. However, the SOD activity was significantly reduced at a concentration of 0.25 g m^{-2} of Asp-SSD-APG and free SSD compared to Asp-SSD ($P < 0.05$, Fig. 6c). Meanwhile, CAT activity was significantly reduced after treatment with a concentration of 0.25 g m^{-2} of Asp-SSD (27.32%), Asp-SSD-APG (19.63%), and free SSD (17.29%) at 72 h when compared to CK ($P < 0.05$). Additionally, CAT activity was concentration-dependent, with higher concentrations resulting in lower viability (Fig. 6d).

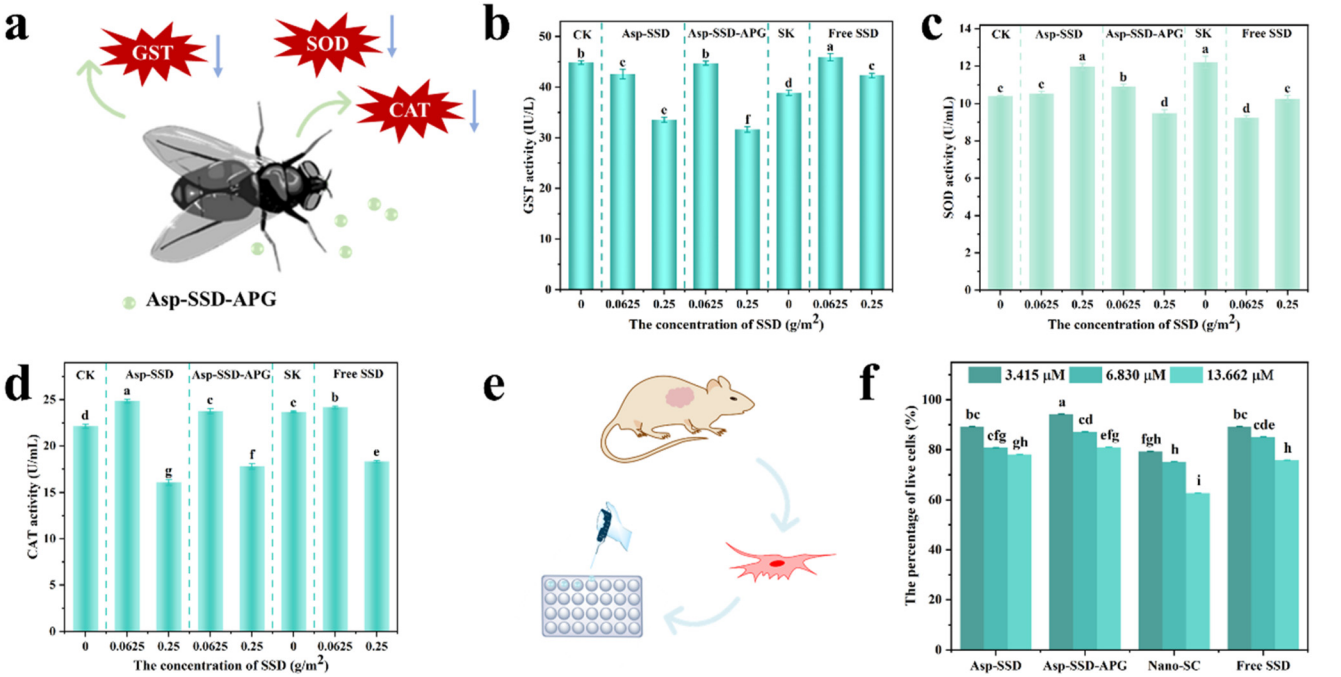

Fig. 6 Schematic diagram of enzyme activities in the control of *M. domestica* (a); Enzyme activity assays of glutathione *S*-transferase (GST) (b), superoxide dismutase (SOD) (c), and catalase (CAT) (d); Schematic diagram of cell viability (e) and cell viability after exposure to insecticides at three concentrations (f). CK: water, SK: 0.1% Tween-80 solution, and free SSD (with 0.1% Tween-80 solution). Bars with the same letters are not significantly different according to Tukey's *post hoc* comparisons at $P < 0.05$.

Various environmental stresses disrupt the normal metabolic processes of the cell, which may lead to large production of radical oxygen species (ROS). The antioxidant activities (SOD and CAT) protect cells against the toxic effects of superoxide radicals.[42] SOD can convert superoxide radicals to peroxide, and CAT detoxifies peroxide to oxygen and water.[43] In Asp-SSD-APG-treated *M. domestica*, we observed a significant decrease in SOD and CAT activities, which might increase the toxic effect of SSD on *M. domestica* (Fig. 6c and d). GST, a vital enzyme of cellular detoxification systems, is of great significance in antioxidant protection and xenobiotic metabolism.[44] In the present study, the GST activity was decreased in *M. domestica* that were exposed to both SSD concentrations of Asp-SSD and Asp-SSD-APG (Fig. 6b). A similar trend was observed for GST activity of the vector tick after treatment with *Cinnamomum verum* and *Origanum vulgare* for 24 h.[45]

Cell viability

The 4T1 cell line from mouse breast cancer that was obtained from the School of Agricultural Sciences of Zhengzhou University was used to investigate the potentially harmful effect of Asp-SSD and Asp-SSD-APG on the cell (Fig. 6e). As shown in Fig. 6f, cell viability was dependent on the concentration of the samples. As the concentration increased, the cell viability of the sample decreased. Similarly, Yang *et al.* reported that SSD caused a concentration- and time-dependent decrease in the cell viability of HEK293 and HepG2 cells.[46] Furthermore, except for the high concentrations of Asp-SSD and free SSD, the cell viability of Asp-SSD, Asp-SSD-APG and free SSD was higher than 80%, and the cell viability of Nano-SC was less than 80%. At low concentrations, no significant change was observed in the percentage of live cells treated with Asp-SSD when compared with free SSD; however, that of the group treated with a low concentration of Nano-SC decreased. Expectedly, the low concentration of Asp-SSD-APG had a high cell viability rate. At a higher concentration, Nano-SC had the lowest cell viability (62.78%) and was significantly different from Asp-SSD, Asp-SSD-APG, and free SSD. This may be due to the addition of multiple surfactants resulting in increased cytotoxicity of the formulation.[47] These results indicated that among all samples, Asp-SSD-APG had the lowest toxic effect on the 4T1 cells. According to the literature, sugar-based surfactants are usually milder on the skin compared to other emulsifier classes.[48] In this study, APG contributed to improving the cell viability of the Asp-SSD system.

Conclusions

In summary, an Asp-SSD self-assembled nanobiopesticide was successfully constructed based on two small molecules SSD and Asp without involving any organic solvents. The preparation conditions were optimized by designing the influences of reactant ratio, temperature, and types of surfactants on the assembly rate and storage stability of Asp-SSD. The results showed that the optimized conditions were a mass ratio of Asp to SSD of 1 : 2 and a reaction temperature of 35 °C in an aqueous solution containing the surfactant APG. The formation mechanism of Asp-SSD was investigated by ITC. The combination of Asp with SSD was through hydrogen bonding and van der Waals interactions. The particle sizes of Asp-SSD and Asp-SSD-APG were 201 nm and 194 nm, respectively. In addition, the surfactant APG could contribute to improving the storage stability and photostability of the Asp-SSD solution. Bioactivity assays showed that Asp-SSD-APG exhibited good quick-acting performance against *M. domestica* in the spray assay, and the insecticidal activities of Asp-SSD and Asp-SSD-APG were better than those of SSD Nano-SC. The cell viability evaluation in 4T1 cells showed that Asp-SSD-APG posed a low risk to the mammalian cells. Compared to CK, Asp-SSD-APG reduced the activity of GST, SOD, and CAT, which contributed to the enhanced insecticidal effect of SSD. Moreover, this facile preparation strategy could be expanded to other natural amino acids, such as glutamic acid. A high assembly rate of 93.95% was achieved (Fig. S7†). This work provides a promising approach to develop a water-based nano-delivery pesticide system by a combination of self-assembly and carrier-minimized technologies, which is of great potential for promoting efficient resource utilization and green development of the public health field.

Experimental

Further details on materials and characterization methods are available in the ESI.†

Preparation of spinosad nanoformulations

Small molecules Asp and SSD at different mass ratios (1 : 1, 1 : 2, or 1 : 4) or different molar ratios (11 : 2, 11 : 4, or 11 : 8) were added simultaneously to 20 mL of deionized water. The concentration of SSD used in the system was 1% of the final nanobiopesticide solution. Afterward, the mixture solution was stirred with a speed of 1000 rpm at 35 °C for 2 h. The supernatant was obtained by centrifugation for the self-assembled product. To stabilize the self-assembled system, surfactants were used. Surfactants were added to the above solution and stirred at room temperature with a speed of 500 rpm for half an hour to obtain the target product. To determine the assembly rate of Asp-SSD and Asp-SSD-APG, 1 mL of sample was set into a 10 mL volumetric flask containing methanol. The solution was sonicated continuously at room temperature for 0.5 h to ensure complete dissolution. Then, the concentration of the solution was measured by high-performance liquid chromatography. The assembly rate of the self-assembled products was calculated according to previous literature.[21]

$$\text{Assembly rate}/\% = \frac{M_t}{M_0} \times 100\%$$

where M_0 represents the initial amount of SSD and M_t represents the amount of SSD in the supernatant.

Author contributions

Huiping Chen: conceptualization, investigation, data curation, methodology, formal analysis, writing – original draft, and writing – review & editing. Zhifei Yang: investigation and validation. Qing Yin: resources and validation. Wenjie Shangguan: software and data curation. Chong Cao: visualization. Qiliang Huang: funding acquisition and project administration. Lidong Cao: conceptualization, supervision, and writing – review & editing.

Data availability

Data will be made available on request. The data supporting this article have been included as part of the ESI.†

Conflicts of interest

There are no conflicts to declare.

Acknowledgements

The authors are grateful for the support from the National Key Research and Development Program of China (2022YFD1700500).

References

1 F. Khamesipour, K. B. Lankarani, B. Honarvar and T. E. Kwenti, *BMC Public Health*, 2018, **18**, 1049.
2 H. M. Kariithi, I. K. Meki, D. G. Boucias and A. M. M. Abd-Alla, *Curr. Opin. Insect Sci.*, 2017, **22**, 71–78.
3 E. Abbasi, Z. Yazdani, S. Daliri and M. D. Moemenbellah-Fard, *Parasite Epidemiol. Control*, 2023, **22**, e00310.
4 S. M. M. Mohafrash, S. A. Fallatah, S. M. Farag and A.-T. H. Mossa, *Ind. Crops Prod.*, 2020, **157**, 112944.
5 M. S. Ayilara, B. S. Adeleke, S. A. Akinola, C. A. Fayose, U. T. Adeyemi, L. A. Gbadegesin, R. K. Omole, R. M. Johnson, Q. O. Uthman and O. O. Babalola, *Front. Microbiol.*, 2023, **14**, 1258968.
6 D. Wang, N. B. Saleh, A. Byro, R. Zepp, E. Sahle-Demessie, T. P. Luxton, K. T. Ho, R. M. Burgess, M. Flury, J. C. White and C. Su, *Nat. Nanotechnol.*, 2022, **17**, 347–360.
7 S. Kumar, M. Nehra, N. Dilbaghi, G. Marrazza, A. A. Hassan and K. H. Kim, *J. Controlled Release*, 2019, **294**, 131–153.
8 M. Kah, R. S. Kookana, A. Gogos and T. D. Bucheli, *Nat. Nanotechnol.*, 2018, **13**, 677–684.
9 W. Shangguan, Q. Huang, H. Chen, Y. Zheng, P. Zhao, C. Cao, M. Yu, Y. Cao and L. Cao, *Nano-Micro Lett.*, 2024, **16**, 193.
10 W. Zhang, S. He, Y. Liu, Q. Geng, G. Ding, M. Guo, Y. Deng, J. Zhu, J. Li and Y. Cao, *ACS Appl. Mater. Interfaces*, 2014, **6**, 11783–11790.
11 L. Huang, S. Zhao, F. Fang, T. Xu, M. Lan and J. Zhang, *Biomaterials*, 2021, **268**, 120557.
12 E. L. Etter, K. C. Mei and J. Nguyen, *Adv. Drug Delivery Rev.*, 2021, **179**, 113994.
13 Y. Tian, G. Tang, Y. Gao, X. Chen, Z. Zhou, Y. Li, X. Li, H. Wang, X. Yu, L. Luo and Y. Cao, *ACS Appl. Mater. Interfaces*, 2022, **14**, 10055–10067.
14 G. Tang, Y. Tian, J. Niu, J. Tang, J. Yang, Y. Gao, X. Chen, X. Li, H. Wang and Y. Cao, *Green Chem.*, 2021, **23**, 2531–2540.
15 H. A. Khan, W. Akram and S. A. Shad, *Acta Trop.*, 2014, **130**, 148–154.
16 P. Piner and N. Üner, *Environ. Toxicol.*, 2014, **29**, 253–260.
17 J. Nguyen, R. Ghazali, P. Batterham and T. Perry, *Pest Manage. Sci.*, 2021, **77**, 3777–3786.
18 T. C. Sparks, G. D. Crouse and G. Durst, *Pest Manage. Sci.*, 2001, **57**, 896–905.
19 V. S. V. Santos and B. B. Pereira, *J. Toxicol. Environ. Health, Part B*, 2020, **23**, 13–26.
20 G. D. Thompson, R. Dutton and T. C. Sparks, *Pest Manage. Sci.*, 2000, **56**, 696–702.
21 Y. Tian, G. Tang, Y. Li, Z. Zhou, X. Chen, Y. Gao, J. Niu, J. Yang, J. Tang, Y. Zhang, X. Zhang and Y. Cao, *Green Chem.*, 2021, **23**, 4882–4891.
22 K. Wei, Z. Li, Z. Zheng, Y. Gao, Q. Huang, M. H. Li and J. Hu, *Adv. Funct. Mater.*, 2024, **34**, 2315493.
23 Z. Li, M. H. Matus, H. A. Velazquez, D. A. Dixon and C. J. Cassady, *Int. J. Mass Spectrom.*, 2007, **265**, 213–223.
24 A. Okamura, T. Hirai, M. Tanihara and T. Yamaoka, *Polymer*, 2002, **43**, 3549–3554.
25 M. J. Rosen and S. B. Sulthana, *J. Colloid Interface Sci.*, 2001, **239**, 528–534.
26 Y. Zhou, X. Yang, L. Bai, Z. Wu, J. Zhang, Z. Qin and J. Fan, *J. Mol. Liq.*, 2022, **368**, 120630.
27 P. G. Righetti, C. Gelfi, A. Bossi, E. Olivieri, L. Castelletti, B. Verzola and A. V. Stoyanov, *Electrophoresis*, 2000, **21**, 4046–4053.
28 Y. Hou, L. Zou, Q. Li, M. Chen, H. Ruan, Z. Sun, X. Xu, J. Yang and G. Ma, *Mater. Today Bio*, 2022, **15**, 100327.
29 C. M. Keck, A. Kovačević, R. H. Müller, S. Savić, G. Vuleta and J. Milić, *Int. J. Pharm.*, 2014, **474**, 33–41.
30 X. Zhao, G. Yu, J. Li, Y. Feng, L. Zhang, Y. Peng, Y. Tang and L. Wang, *ACS Sustainable Chem. Eng.*, 2018, **6**, 4105–4114.
31 Y. Fang, Z. Xie, H. Zhang, Q. Xiong, B. Yu, J. Cheng, W. Shang and J. Zhao, *J. Controlled Release*, 2024, **367**, 837–847.
32 P. D. Ross and S. Subramanian, *Biochemistry*, 1981, **20**, 3096–3102.
33 Q. Jiang, Z. Lin, M. Peng, B. Zhou, E. Liu, Z. Li, Y. Wei, H. Yang, F. Song, M. Yin, J. Shen and S. Yan, *ACS Appl. Nano Mater.*, 2023, **6**, 13524–13532.
34 G. B. Li, J. Wang and X. P. Kong, *Carbohydr. Polym.*, 2020, **249**, 116865.
35 M. M. A. El-Sukkary, N. A. Syed, I. Aiad and W. I. M. El-Azab, *J. Surfactants Deterg.*, 2008, **11**, 129–137.

36 Y. Wu, J. Yu, X. Ma and J. Zhang, *Chin. Chem. Lett.*, 2007, **18**, 1173–1175.
37 S. Shrestha, B. Wang and P. Dutta, *Adv. Colloid Interface Sci.*, 2020, **279**, 102162.
38 J. Wan, Y. Kim, M. J. Mulvihill and T. K. Tokunaga, *Environ. Toxicol. Chem.*, 2018, **37**, 1301–1308.
39 Y. Li, Y. Zhang, L. Zhan, J. Hou and B. Li, *Tenside, Surfactants, Deterg.*, 2023, **60**, 245–252.
40 R. L. Thurlkill, G. R. Grimsley, J. M. Scholtz and C. N. Pace, *Protein Sci.*, 2006, **15**, 1214–1218.
41 E. Dong, Z. Yang, C. Zhou, C. Wang, S. Li, Q. Ouyang, L. Kong, Z. He, J. Xie, P. Li and P. Yang, *React. Funct. Polym.*, 2019, **141**, 123–132.
42 N. Schvezov, G. A. Lovrich, F. Tapella and M. C. Romero, *Comp. Biochem. Physiol., Part A: Mol. Integr. Physiol.*, 2013, **164**, 605–611.
43 Y. Li, L. Wei, J. Cao, L. Qiu, X. Jiang, P. Li, Q. Song, H. Zhou, Q. Han and X. Diao, *Chemosphere*, 2016, **144**, 234–240.
44 D. Gweshelo, R. Muswe and S. Mukanganyama, *BMC Complementary Altern. Med.*, 2016, **16**, 238.
45 Y. Qiao, Z. Yu, L. Bai, H. Li, S. Zhang, J. Liu, Z. Gao and X. Yang, *Ecotoxicol. Environ. Saf.*, 2021, **224**, 112672.
46 M. Yang, G. Xiang, D. Li, Y. Zhang, W. Xu and L. Tao, *Mutat. Res., Genet. Toxicol. Environ. Mutagen.*, 2016, **812**, 12–19.
47 J. Feng, Y. Ma, Z. Chen, Q. Liu, J. Yang, Y. Gao, W. Chen, K. Qian and W. Yang, *ACS Sustainable Chem. Eng.*, 2021, **9**, 4988–4999.
48 S. Savić, S. Tamburić and M. M. Savić, *Expert Opin. Drug Delivery*, 2010, **7**, 353–369.